

## **Metal-organic frameworks constructed from a tetrahedral silicon-based linker for selective adsorption of methylene blue**

Yuan-Feng Hui,<sup>acd</sup> Chun-Li Kang,<sup>a</sup> Tao Tian,<sup>\*a</sup> Chao-Ying Gao,<sup>\*b</sup> Jing Ai,<sup>d</sup> Chao Liu,<sup>d</sup> Hong-Rui Tian,<sup>d</sup>  
S. Dang<sup>\*d</sup> and Zhong-Ming Sun

<sup>a</sup>College of Environment and Resources, Jilin University.

<sup>b</sup>College of Chemistry and Chemical Engineering, Inner Mongolia University for the Nationalities,  
Tongliao 02800, PR China.

<sup>c</sup>Jilin Institute Of Chemical Technology

<sup>d</sup>State Key Laboratory of Rare Earth Resource Utilization, Changchun Institute of Applied  
Chemistry, Chinese Academy of Sciences, 5625 Renmin Street, Changchun, Jilin 130022, China.

Table S1. Selected bond lengths for **1**

<b>1</b>			
Cd(1)-O(2)	2.203(4)	C(8)-Cd(1)#8	2.726(7)
Cd(1)-O(2)#1	2.203(4)	O(3)-Cd(2)#7	2.323(5)
Cd(1)-O(3)#2	2.367(5)	O(3)-Cd(1)#8	2.367(5)
Cd(1)-O(3)#3	2.367(5)	Cd(2)-O(1)#4	2.280(4)
Cd(1)-O(4)#2	2.389(5)	O(4)-Cd(1)#8	2.389(5)
Cd(1)-O(4)#3	2.389(5)	Cd(2)-O(3)#5	2.323(5)
Cd(1)-C(8)#2	2.726(7)	Cd(2)-O(3)#3	2.323(5)
Cd(1)-C(8)#3	2.726(7)	Cd(2)-O(1W)#4	2.227(6)
Cd(2)-O(1W)	2.227(6)	Cd(2)-O(1)	2.280(4)

Symmetry transformations used to generate equivalent atoms: #1  $-x+1, y, -z+1/2$ ; #2  $x-1/2, y-1/2, z-1$ ; #3  $-x+3/2, y-1/2, -z+3/2$ ; #4  $-x+3/2, -y+1/2, -z+1$ ; #5  $x, -y+1, z-1$ ; #6  $-x+1, y, -z+3/2$ ; #7  $-x+3/2, y+1/2, -z+3/2$ ; #8  $x+1/2, y+1/2, z+1$ .

Table S2. Selected bond lengths for **2**

<b>2</b>			
Co(1)-O(1)	2.000(2)	Co(1)-O(5)#1	2.063(3)
Co(1)-N(2)#2	2.070(3)	Co(1)-O(11)	2.125(2)
Co(1)-O(9)#2	2.128(2)	Co(1)-O(3)#2	2.191(3)
Co(2)-O(9)	1.964(2)	Co(2)-O(7)#3	1.964(2)
Co(2)-O(4)	1.995(2)	Co(2)-N(7)#4	2.020(3)
Co(3)-O(6)#5	2.047(3)	Co(3)-O(10)	2.071(3)
Co(3)-O(9)	2.091(2)	Co(3)-O(12)	2.107(3)
Co(3)-O(13)	2.170(3)	Co(3)-N(1)	2.190(3)
N(7)-Co(2)#7	2.020(3)	O(3)-Co(1)#6	2.191(3)
O(5)-Co(1)#8	2.063(3)	O(7)-Co(2)#10	1.964(2)
O(6)-Co(3)#9	2.047(3)	O(9)-Co(1)#6	2.128(2)

Symmetry transformations used to generate equivalent atoms: #1  $-x+1, y-1/2, -z+3/2$ ; #2  $x-1, y, z$ ; #3  $-x+2, y-1/2, -z+5/2$ ; #4  $x+1, -y+1/2, z+1/2$ ; #5  $-x+2, y-1/2, -z+3/2$ ; #6  $x+1, y, z$ ; #7  $x-1, -y+1/2, z-1/2$ ; #8  $-x+1, y+1/2, -z+3/2$ ; #9  $x+2, y+1/2, -z+3/2$ ; #10  $-x+2, y+1/2, -z+5/2$

Table S3. Selected bond lengths for **3**

<b>3</b>			
Zn(1)-O(2)	1.986(3)	Zn(1)-O(6)#1	1.993(3)
Zn(1)-O(8)#2	2.021(3)	Zn(1)-O(9)	2.064(3)
Zn(1)-O(2W)	2.102(3)	Zn(2)-O(1)	1.994(3)
Zn(2)-O(7)#2	2.011(3)	Zn(2)-O(1W)	2.075(4)
Zn(2)-O(9)	2.111(3)	Zn(2)-O(3)#3	2.166(3)
Zn(2)-O(4)#3	2.275(4)	Zn(2)-C(8)#3	2.560(5)
Zn(3)-O(9)	1.944(3)	Zn(3)-N(5)#4	1.988(4)
Zn(3)-O(5)#1	1.996(3)	Zn(3)-N(3)	2.008(4)
O(3)-Zn(2)#5	2.166(3)	O(4)-Zn(2)#5	2.275(4)
O(5)-Zn(3)#6	1.996(3)	O(7)-Zn(2)#7	2.011(3)
O(6)-Zn(1)#6	1.993(3)	O(8)-Zn(1)#7	2.021(3)
N(5)-Zn(3)#8	1.989(4)		

Symmetry transformations used to generate equivalent atoms: #1  $x-1/2, -y+1/2, z+1/2$ ; #2  $x+1/2, -y+1/2, z+1/2$ ; #3  $x, y+1, z$ ; #4  $x+1/2, -y+3/2, z+1/2$ ; #5  $x, y-1, z$ ; #6  $x+1/2, y+1/2, z-1/2$ ; #7  $x-1/2, -y+1/2, z-1/2$ ; #8  $x-1/2, -y+3/2, z-1/2$ .

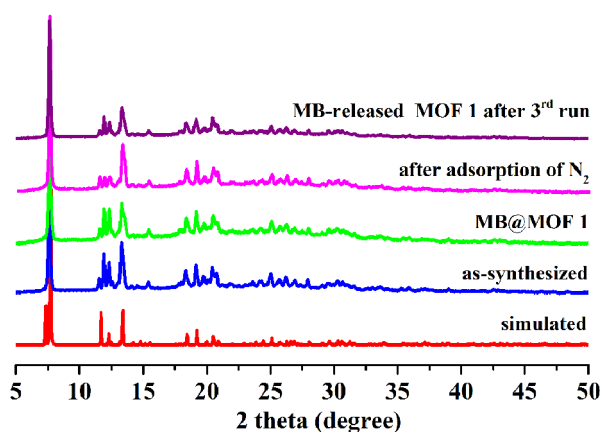


Figure S1 PXRD patterns for MOF 1: simulated MOF 1, as-synthesized MOF 1, MB@MOF 1, MB-released MOF 1 after 3<sup>rd</sup> run, and MOF 1 after N<sub>2</sub> adsorption.

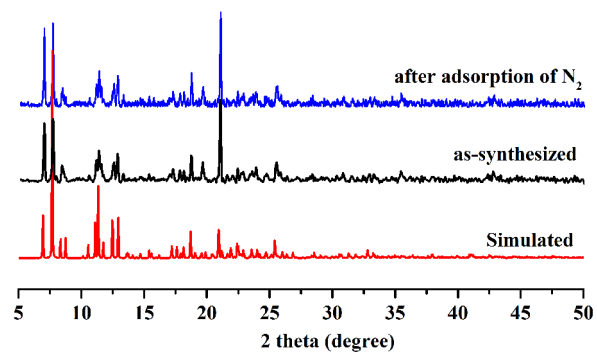


Figure S2 Experimental and simulated PXRD patterns of MOF **2**, as well as that of the sample after adsorption of  $N_2$ .

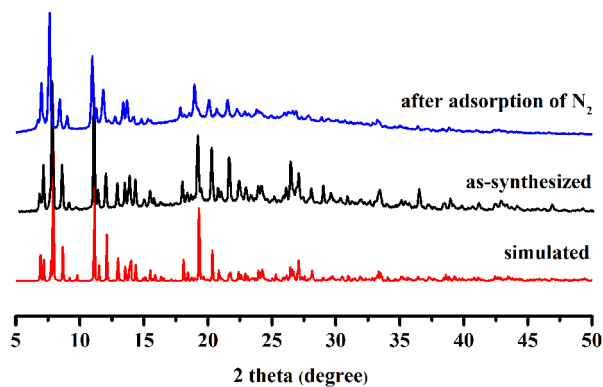


Figure S3 Experimental and simulated PXRD patterns of MOF **3**, as well as that of the sample after adsorption of  $N_2$ .

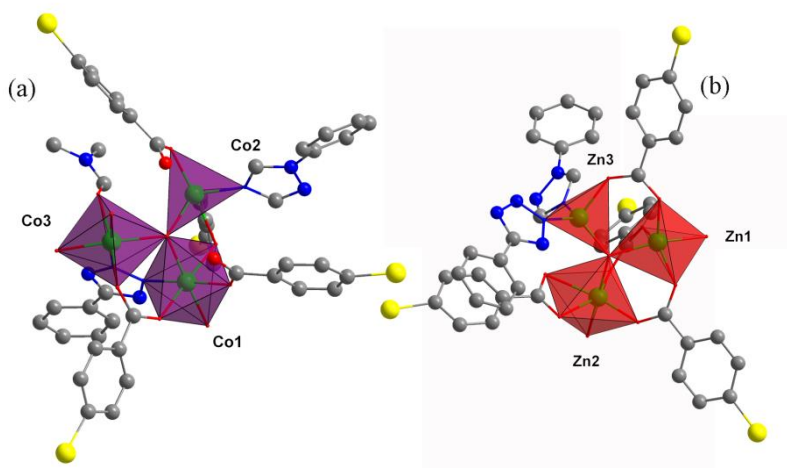


Figure S4 The trinuclear SBUs in compounds **2** (a) and **3** (b).

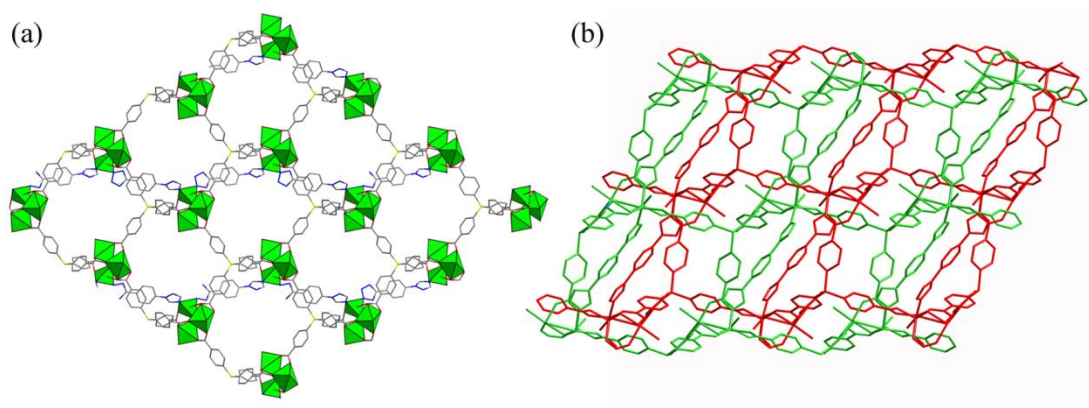


Figure S5 A view of the single network along  $a$ -axis (a) and the 2-fold interpenetrating 3D architecture along the  $b$ -axis (b) in **3**.

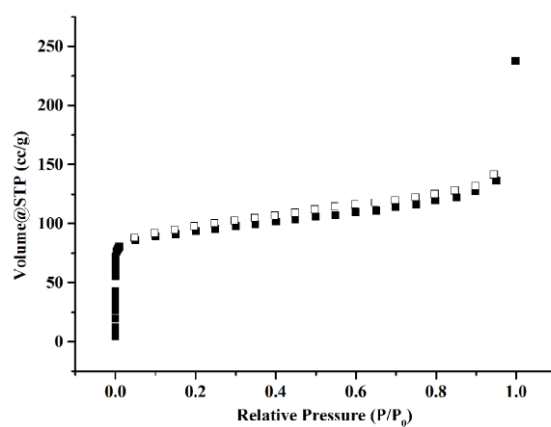


Figure S6  $N_2$  sorption isotherms for MOF-1 at 77 K to 1 bar.

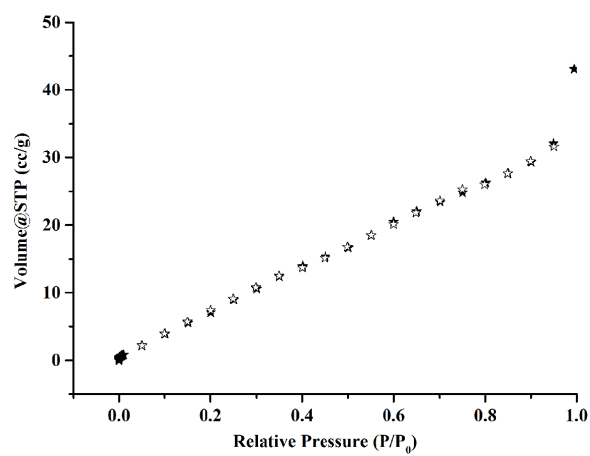


Figure S7  $N_2$  sorption isotherms for MOF-2 at 77 K to 1 bar.

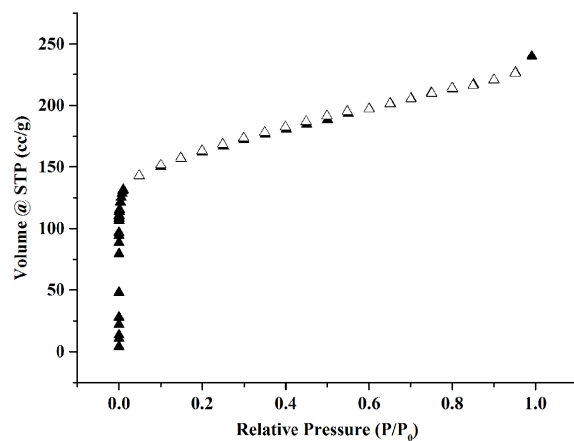


Figure S8 N<sub>2</sub> sorption isotherms for MOF-3 at 77 K to 1 bar.

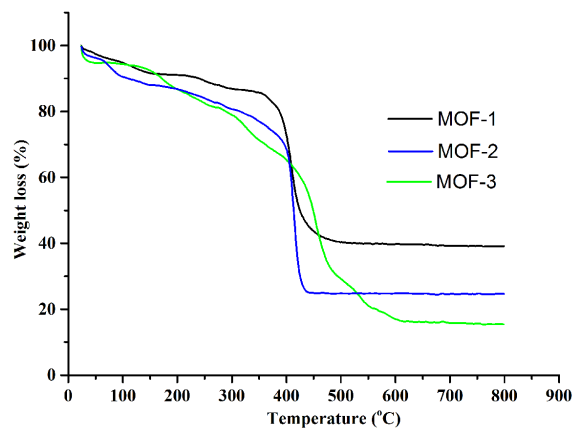


Figure S9 The TGA curves of the three compounds.

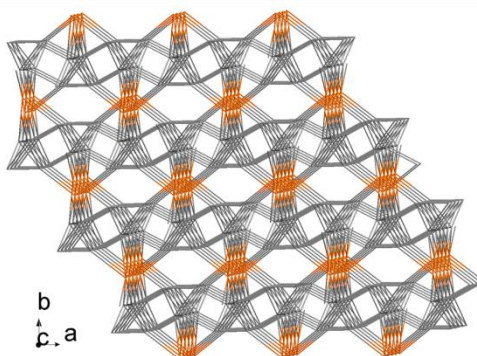


Figure S10 The simplified (4, 4, 4)-connected topological net analyzed using TOPOS software.

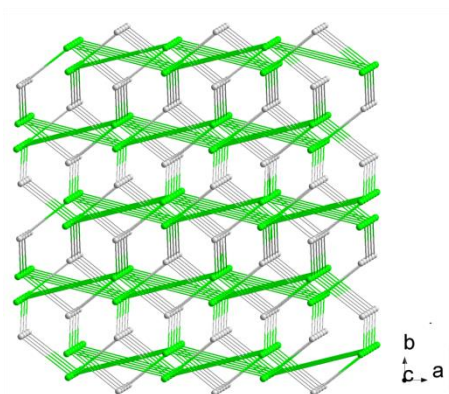


Figure S11 The simplified (4, 6)-connected topological net analyzed using TOPOS software.

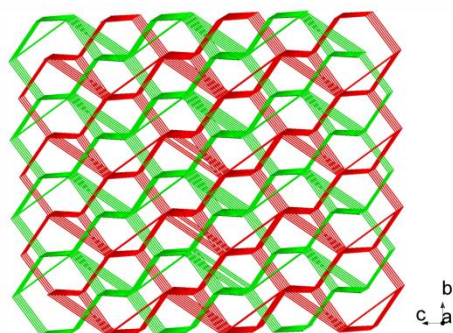
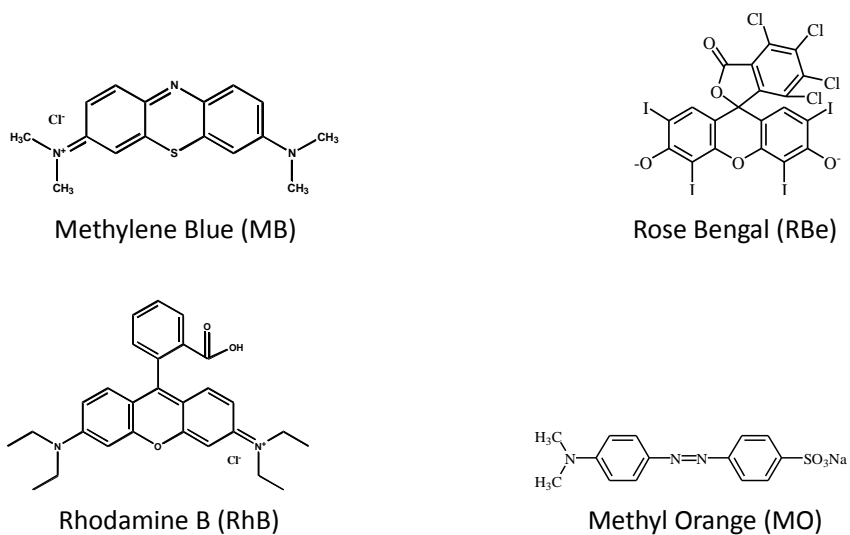


Figure S12 The simplified (4, 6)-connected topological net with two-fold interpenetration analyzed using TOPOS software.



Scheme S1 Chemical structures of organic dyes used in this work. Herein, the sizes of MB and MO molecular are provided for comparison considering their similarity in shapes:  $4.59 \times 8.01 \times 16.75 \text{ \AA}^3$  for MB and  $5.31 \times 7.25 \times 17.39 \text{ \AA}^3$  for MO.

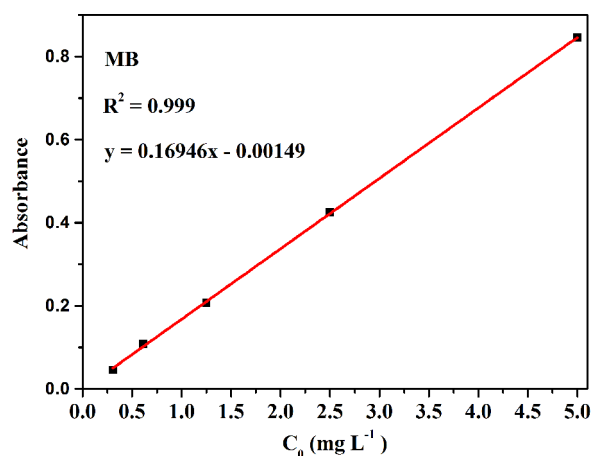


Figure S13 The absorbed intensity (black dots) of MB dye in different concentrations ( $C_0 = \text{mg L}^{-1}$ ). The red solid line is the best linear fit.

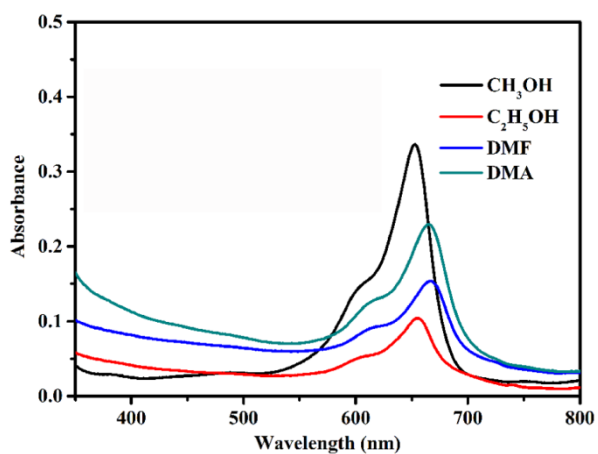


Figure S14 UV-vis spectroscopic analyses of MB solution after dye-releasing experiments using different elution solvents.

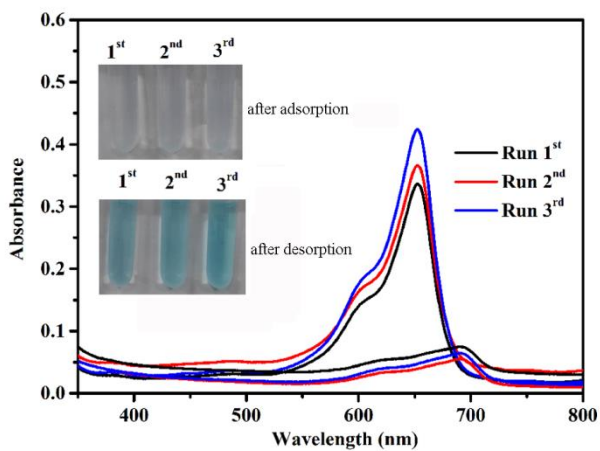


Figure S15 The UV-vis spectra of MB solution measured based on three adsorption-desorption cycles. Inset: the photographic images of MB solutions after adsorption (top) and desorption

(bottom) experiments.

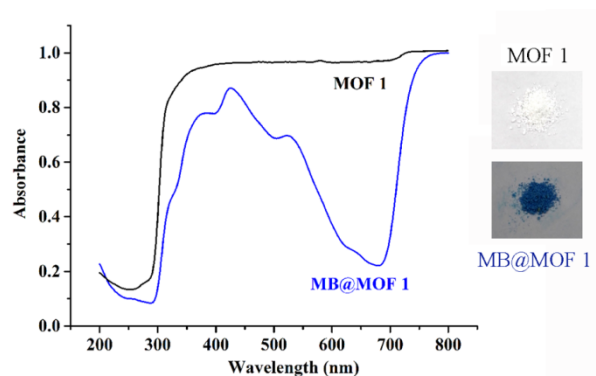


Figure S16 Solid state UV-vis spectra of MOF 1 and the composite MB@MOF 1, as well as their photographic images.

Table S4 Comparison of adsorption time for MOF-based adsorbents, corresponding to the materials in Table 1 in the text.

\*: the provided concentration in the literature is  $0.03 \text{ mmol L}^{-1}$ , and the value is equivalent to about  $11.2 \text{ mg L}^{-1}$ .

Materials	Quality of adsorbent (mg)	Concentration of MB ( $\text{mg L}^{-1}$ )	Volume of MB (mL)	Time	Adsorption percentage (%)	Ref.
FJI-C2	10	11.2*	10	60 min	90	17
$^a[\text{Ca}(\text{HDCPP})_2(\text{H}_2\text{O})_2]_n(\text{DMF})_{1.5n}$	5	20	15	120 min	>99	18
ZJU-24	5	5	50	12 h	>99	19
$^a[\text{Mg}(\text{HDCPP})_2(\text{DMF})_2]_n \cdot (\text{H}_2\text{O})_{7n}$	5	20	15	120 min	>99	18
DUT-23(Cu)	5	20	40	150 min	—	20
Amino-MIL-101-Al	10	50	50	6 h	>99	21
MIL-100 (Fe)	10	30	50	24 h	>99	22
Co-MOF	20	40	2	10 min	—	23
Ni-MOF	20	40	2	10 min	—	23
UMCM-150 flower-like	5	20	40	80 min	—	24
$\text{Cu}_3(\text{BTC})_2$	10	30	10	24 h	—	25
<b>1</b>	5	12	3	40 s	>99	<b>This work</b>

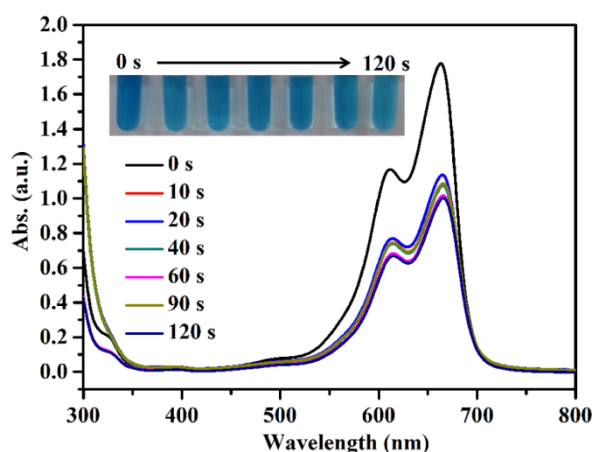
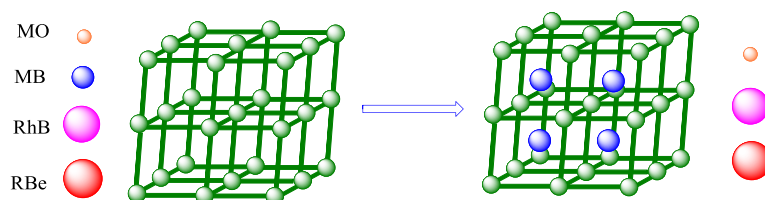


Figure S17. UV/vis spectra of MB dye adsorption with MOF **3**.

MOF **3**: 3 mg; MB solution: 12 mg L<sup>-1</sup>, 3 mL.

Considering that MOF **3** has a larger surface area (594 m<sup>2</sup> g<sup>-1</sup>) than MOF **1** (356 m<sup>2</sup> g<sup>-1</sup>), removal of MB dye on MOF **3** was also investigated. The adsorption details were the same as those on MOF **1**. It was found that the blue solution of MB faded slightly, as shown in the photographic images. Besides, the UV/vis spectrophotometry was utilized to monitor the MB dye concentration, which showed no obvious decrease in absorbance intensity. Compared with MOF **1**, MOF **3** did not show better adsorption performance towards MB dye. This observation may be attributed to the interpenetration in framework **3**. Thereby, the thorough investigation on dye removal with MOF **3** was not carried out.



Scheme S2 Illustration of the size-selectivity adsorption process.